A EUROPEAN JOURNAL OF CHEMICAL BIOLOGY

CHEMBIOCHEM

SYNTHETIC BIOLOGY & BIO-NANOTECHNOLOGY

Accepted Article

Title: Promotion and Inhibition of the Oxidase-mimicking Activity of Nanoceria by Phosphate, Polyphosphate and DNA

Authors: Yilin Zhao, Haotian Li, Anand Lopez, Haijia Su, and Juewen Liu

To be cited as: *ChemBioChem* 10.1002/cbic.202000049

Link to VoR: http://dx.doi.org/10.1002/cbic.202000049

A Journal of ChemPubSoc Europe

WILEY-VCH

www.chembiochem.org

Promotion and Inhibition of the Oxidase-mimicking Activity of Nanoceria by Phosphate, Polyphosphate and DNA

Yilin Zhao [a,b], Haotian Li [a], Anand Lopez [b], Haijia Su*[a] and Juewen Liu*[b]

a Beijing Key Laboratory of Bioprocess, Beijing University of Chemical Technology (BUCT), 15 BeiSanHuan East Road, ChaoYang District, Beijing, 100029, P. R. China. E-mail: suhj@mail.buct.edu.cn

b Department of Chemistry, Waterloo Institute for Nanotechnology, University of Waterloo, Waterloo, Ontario, N2L 3G1, Canada. E-mail: liujw@uwaterloo.ca

Abstract

Nanoceria (CeO_2 nanoparticles) is an extensively studied nanozyme with interesting oxidase-mimicking activity. Since it can work in the absence of toxic and unstable H_2O_2, CeO_2 nanoparticles has been widely used in biosensing. CeO_2 nanoparticles often encounters phosphate containing molecules that may affect its catalytic activity and various reports exist in the literature showing both promoted and inhibited activity. In this work, we systematically studied five types of phosphates including orthophosphate, pyrophosphate, triphosphate, a polyphosphate with 25 phosphate units (Pi_{25}), and also DNA oligonucleotides of various lengths and sequences. DNA was included since it contains a phosphate backbone that can strongly adsorb on nanoceria. We observed inhibited activity by a high concentration of DNA in acetate buffer, while increased activity was achieved by a low concentration of DNA in phosphate buffer. These discoveries provide an important understanding for further use of CeO_2 nanoparticles in biosensor development, materials science, and nanotechnology.

Keywords: nanozymes; DNA; oxidase; CeO_2; biosensors

Introduction

The word nanozyme was coined to describe nanomaterial-based enzyme mimics.[1-4] This field took off with the discovery of the peroxidase-mimicking activity of iron oxide nanoparticles.[5] In fact, many nanozymes are metal oxides, such as CeO_2,[6-9] MnO_2,[10] and NiO.[11-12] Nanoceria (CeO_2 nanoparticle) containing mixed valence state (Ce^{3+}, Ce^{4+}) is a particularly versatile nanozyme with a diverse range of activities mimicking oxidase,[6, 13] catalase,[14] superoxide dismutase,[15] photolyase,[16] phosphatase,[17] and nuclease.[18] Its oxidase-like activity is attractive since unstable and toxic H_2O_2 is not required for the reactions.[19-20]

Nanoparticles exhibit a high specific surface area affording a high capacity to adsorb various small molecules and polymers such as amino acids, proteins, DNA, and ions present in biological media.[21] Nanozymes have been interfaced with biomolecules and biopolymers for various reasons including sensing and therapeutic applications.[22-24] For example, fluoride can improve the oxidase-like activity of CeO_2 nanoparticles,[13, 25-26] allowing highly sensitive and selective detection of F^-. Nanoparticles often encounter phosphate and phosphate containing molecules in biological media and buffers. DNA has a phosphate backbone,[27] and most lipids also contain a phosphate group.[28]

Phosphate was reported to shift the redox state of CeO_2 nanoparticles,[21] and a few phosphate containing molecules were reported to affect its oxidase-like activity (Table S1). For example, we reported that a high concentration of DNA oligonucleotide moderately inhibited the oxidation of TMB.[29] Yang et al showed that DNA increased the activity of CeO_2 nanoparticles and nanocubes for ABTS oxidation, but inhibited the activity of CeO_2 nanorods.[30] In two studies, PCR products (duplex DNA) inhibited CeO_2 activity.[31-32] Qu and coworkers reported that adding guanosine triphosphate (GTP) accelerated the oxidation of ABTS.[33] Andreescu and coworkers showed that the aptamer of ochratoxin A (OTA) can accelerate TMB oxidation by CeO_2.[34] These reports appeared to be inconsistent regarding the effect of DNA or nucleotides on the activity of CeO_2, and we noticed that different substrates and buffers were used.

We suspected that the effect of DNA could be affected by its concentration and sequence, while salt concentration, buffer, pH, and the type of substrate may also play a role. We recently studied the adsorption of various phosphate and polyphosphate on nanoceria.[35-36] In general, when a

molecule has more terminal phosphate groups (instead of bridging phosphate), its affinity to CeO_2 is higher.[36] In this work, we systematically study the effect of phosphate and polyphosphate to rationalize the previous studies. This work articulates that care is needed to specify and compare the experimental conditions for nanozyme-based sensors.

■ MATERIALS AND METHODS

Chemicals. All the DNA samples were purchased from Integrated DNA Technologies (IDT, Coralville, IA, USA, see Table S2 for sequence). Sodium acetate and sodium hydroxide were purchased from Mandel Scientific (Guelph, Ontario, Canada). Nanoceria (catalog number 289744, 20 wt% dispersed in 2.5% acetic acid), 3, 3′, 5, 5′-tetramethylbenzidine (TMB), 2, 2′-azino-bis (3-ethylbenzothiazoline-6-sulfonic acid) diammonium salt (ABTS), sodium dihydrogen phosphate (Pi), sodium pyrophosphate (PPi), sodium trimetaphosphate (STMP), sodium triphosphate (STPP), sodium polyphosphate with 25 phosphate units (Pi_{25}) were purchased from Sigma-Aldrich. Milli-Q water was used to prepare all the buffers and solutions.

Dynamic Light Scattering (DLS) and ζ-potential. Zeta-potential was measured on a Malvern instrument (Zetasizer Nano 90) using the dip-cell setup. In a typical experiment, 100 μg/mL CeO_2 was dispersed in 1 mL buffer of various pH, typically 10 mM phosphate or acetate at 25°C. The hydrodynamic size of the CeO_2 nanoparticles was measured on the same instrument.

Transmission Electron Microscopy (TEM). The morphology and size of nanoceria were investigated by TEM measurement (JEOL 2011 microscope, Japan). Typically, 100 μg/mL of CeO_2 dispersed in a buffer solution (acetate or phosphate buffer, pH 4, 10 mM) containing DNA at designed concentrations was used. These samples were allowed to dry overnight at room temperature before imaging.

Nanoceria-mediated oxidation of ABTS or TMB. Taking 5 nm as the average particle size based on our TEM measurement and the density to be 7.2 g/cm^3 (the same as bulk CeO_2), the molar concentration of nanoceria in the stock was 860 μM. Typically, CeO_2 nanoparticles (100 μg/mL, 430 nM) was suspended in 100 μL of acetate buffer (10 mM, pH 4) containing phosphate species of different concentrations. After incubation for 1 h, a final concentration of 0.5 mM ABTS or TMB

was added to initiate the reaction, and the activity was followed at 420 nm for ABTS, or at 450 nm and 652 nm for TMB.

DNA adsorption and desorption assays. For visual observation, 2 μM Cy3-labeled DNA C_{15} (Cy3-C_{15}) was used and various concentrations of nanoceria were added in 10 mM phosphate buffer (pH 4.0). The samples were observed using Safe Imager™ 2.0 Blue-Light Transilluminator (Life Technologies, exciting at ~470 nm) and recorded using a digital camera. To further study DNA adsorption, Cy3-C_{15} (100 nM) was dissolved in the phosphate buffer. After the free DNA was scanned for 2 min (excitation at 550 nm, emission at 570 nm) using a microplate reader, a small volume of CeO_2 (final concentration 100 μg/mL) was added to induce DNA adsorption. The fluorescence intensity was normalized based on the initial intensity before adding CeO_2. The desorption of DNA was recorded after a quick addition of phosphate to the Cy3-C_{15}/CeO_2 sample.

■ RESULTS AND DISCUSSION

Phosphate, polyphosphate and DNA. The goal of this work is to study the effect of phosphate containing species on the oxidase-like activity of CeO_2 nanoparticles. To have a full understanding, we included a total of five phosphates with various degrees of polymerization including simple inorganic orthophosphate (Pi), pyrophosphate (PPi), triphosphate (STPP), a polyphosphate with 25 phosphate units (Pi_{25}) and a cyclic triphosphate (STMP) (Figure 1a). In addition, DNA oligonucleotides of various lengths and sequences were tested, since DNA has a phosphate backbone and it has been interfaced with CeO_2 although with inconsistent results.[29-32, 34]

We previously systematically characterized the CeO_2 nanoparticles,[26, 37] and these studies are not repeated here. In brief, our CeO_2 had an average size of ~5 nm at pH 4 and ~30 nm at pH 8 in acetate buffer as characterized by dynamic light scattering (Figure 1b). The nanoparticles gradually aggregated when the pH was close to neutral, when the surface charge also became close to zero.

The optimal condition for the oxidation reaction by CeO_2 is pH 4.[6] The bare CeO_2 nanoparticles were positively charged at pH 4 due to the protonation of its surface hydroxyl groups.[13] Adding 100 μM of Pi, PPi, STPP, STMP or Pi_{25} to 100 μg/mL CeO_2 nanoparticles all inversed the charge to negative, indicating adsorption of these species (Figure 1c). Adding 10 μM

of A_{15} DNA to 10 μg/mL CeO_2 achieved the same effect. For comparison, the charge became neutral with 1 mM F^-, while negative charge was achieved only with 5 mM F^-. Since it took more F^- to reverse the charge, F^- had a lower adsorption affinity compared to phosphate and the polyphosphates.[26] We included F^- as a control since it promoted the catalytic activity of CeO_2.[13]

We also gradually titrated Pi and the A_{15} DNA to the CeO_2 (Figure 1d, also see Figure S1 for the same plot on the linear scale). The surface charge became close to zero when the DNA/CeO_2 molar ratio was ~12, while a ratio of close to 200 was needed for Pi/CeO_2. The change of zeta-potential reflected the adsorption process. Since each A_{15} has 14 phosphate bridges, it can explain the lower concentration of DNA needed to neutralize the charge. It is unclear whether all the phosphate bridges in the DNA were attached to the CeO_2 surface, but each bridge contributed to a negative charge.

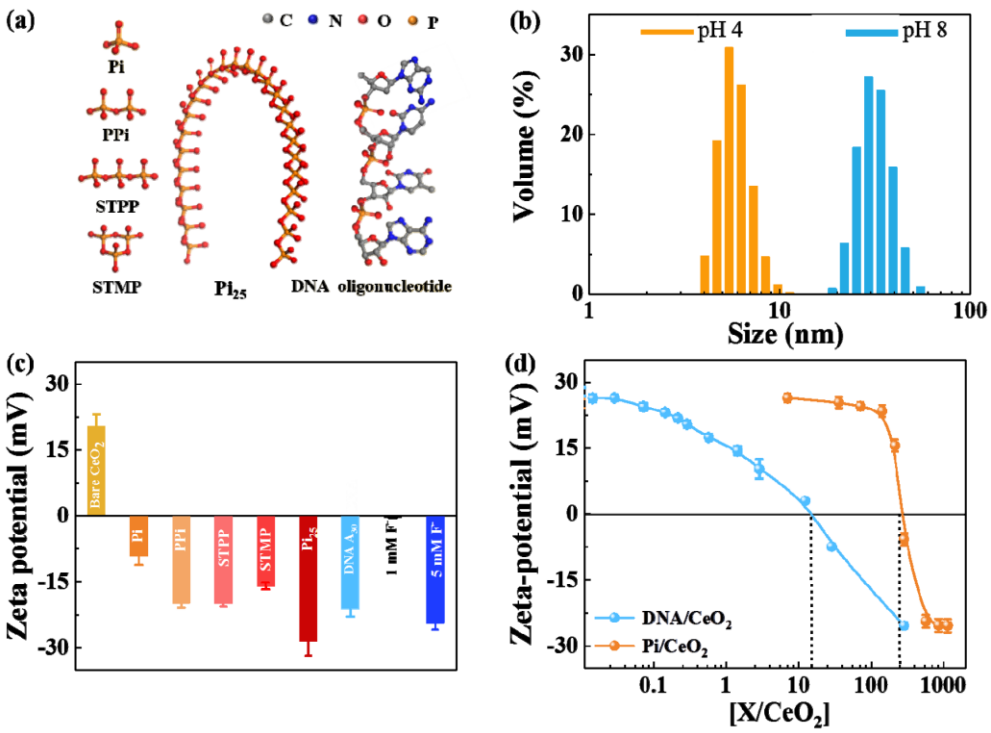

Figure 1. (a) The structures of the phosphate species studied in this work. A 4-mer DNA oligonucleotide is also shown. (b) The hydrodynamic size distribution of the CeO_2 nanoparticles dispersed in acetate buffers (10 mM) of different pH. (c) Zeta-potential of the CeO_2 nanoparticles before and after adding different phosphate species (100 μM each), DNA A_{15} (10 uM) and F^- (1 and 5 mM) in pH 4 acetate buffer (10 mM). (d) Zeta-potential of the CeO_2 nanoparticles as a function of the molar ratio of A_{15} DNA to CeO_2 or Pi to CeO_2 in pH 4 acetate buffer (10 mM). The concentration of the CeO_2 nanoparticles was 100 μg/mL (particle concentration was 430 nM) in all samples, except when the ratio of DNA/CeO_2 was larger than 10, 10 μg/mL of CeO_2 was used.

Phosphate slightly enhanced the oxidation of ABTS. Two chromogenic substrates were studied in this work: TMB and ABTS. ABTS (pK_a 2.2) is negatively charged, while TMB (pK_a=4.3) is partially positively charged at pH 4.0. By studying both substrates, we could learn the effect of electrostatic interactions. We first tested the effect of the phosphate species using negatively charged ABTS in a pH 4 acetate buffer. ABTS has no color, but after oxidation it has a green color with an absorption peak at 420 nm (Figure 2a). We used this peak to quantify its oxidation. The CeO_2 nanoparticles produced a slightly green product, while a deeper green color was observed in the presence of Pi, suggesting an enhancement effect of Pi (inset of Figure 2a). To determine an optimal phosphate concentration, we added various concentrations of Pi, PPi, STMP, STPP or Pi_{25}. Since different species have different phosphate units, to make a fair comparison, we made them all contain the same number of phosphate units in this experiment (e.g. the molar concentration of Pi_{25} was 4% of that Pi) (Figure 2b). We only observed a moderate rate enhancement and the turnover of each CeO_2 nanoparticle was still less than 100 with 10 mM Pi. A similar trend was also observed with PPi, STPP and STMP, while Pi_{25} showed more enhancement. Similar observations were also made when the same molar concentrations of these phosphate species were used (Figure S2a). Note that these phosphates did not have light absorption beyond 250 nm (Figure S3).

We also measured the kinetics of the reactions and F^- was also tested for comparison (Figure 2c, d). With 5 mM F^-, the turnover number reached ~200 in 1 min and 580 in 60 min. The acceleration effect of all the phosphates was much smaller compared to F^-.[13] When fully capped by phosphate, the CeO_2 surface should repel negatively charged ABTS, and this might inhibit the activity. However, phosphate can also inhibit the adsorption of oxidation product,[26] which should promote the turnover of the nanozyme surface. Based on the result, a balance of these two effects resulted in an overall small enhancement. Therefore, these phosphates only moderately enhanced ABTS oxidation, and this effect was especially small for Pi.

10.1002/cbic.202000049

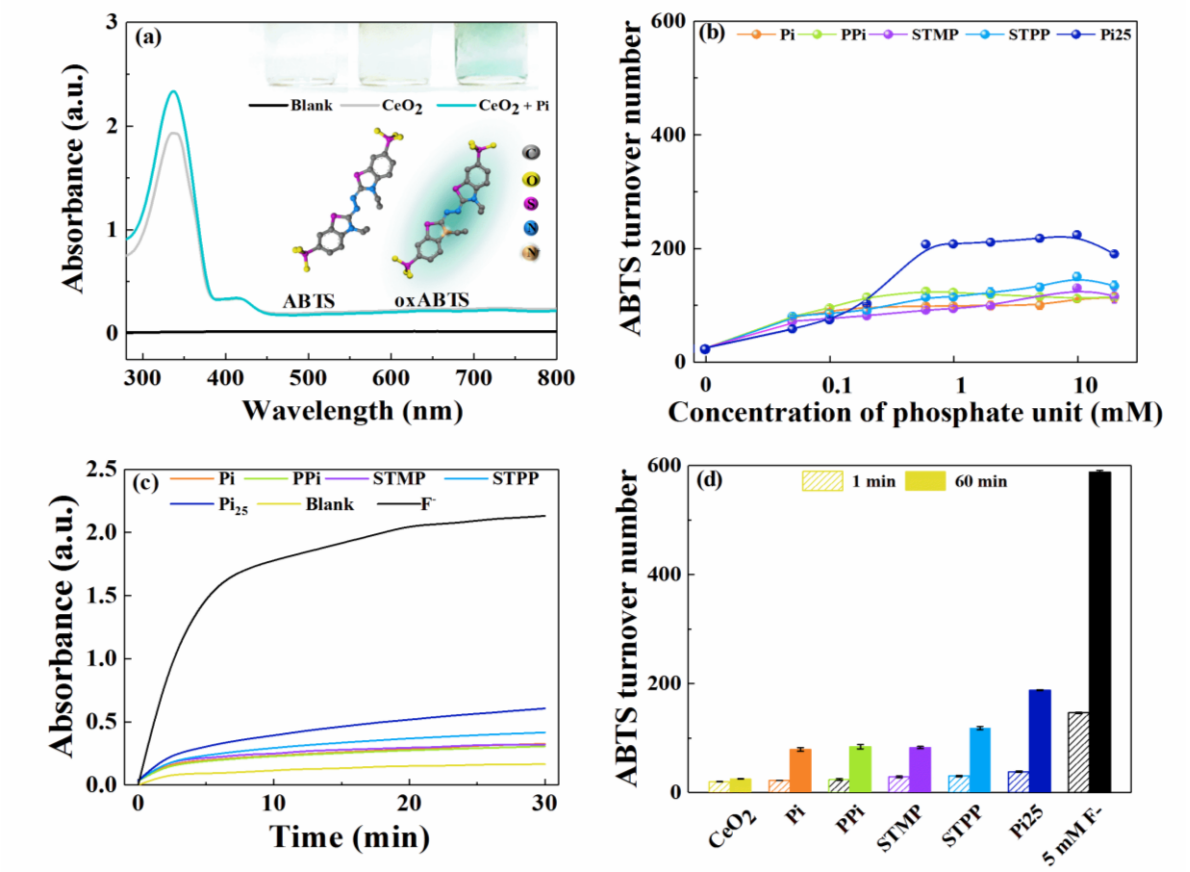

Figure 2. (a) UV-vis spectra of ABTS (420 mM) oxidation by the CeO_2 nanoparticles without or with Pi (10 mM) after 30 min reaction. Inset: the structures and photographs of ABTS before and after oxidation. (b) Turnover number of ABTS oxidation by each CeO_2 nanoparticle in the presence of various concentrations of phosphate after 60 min reaction. The *x*-axis is the concentration of the total phosphate unit. (c) Kinetics of ABTS oxidation with the CeO_2 nanoparticles in the presence of 10 mM total phosphate units of each species. Fluoride (5 mM) was added as a control. (d) Turnover number based on the data in (c) when the reaction time was 1 min and 60 min. ABTS (0.5 mM), CeO_2 nanoparticles (100 μg/mL) and acetate buffer (10 mM, pH 4) were used in all reactions.

Phosphates accelerate the oxidation of TMB more. We then repeated the reaction using TMB. TMB has a two-step oxidation process first forming a one-electron blue product, which could be further oxidized to a two-electron yellow product. We also observed enhanced oxidation by Pi (Figure 3a), and all the phosphate species accelerated the reaction similarly (Figure 3b). As shown in Figure S4, when the concentration of Pi_{25} was over 0.1 mM, the absorption wavelength of the oxidized TMB (oxTMB) blue shifted significantly. Therefore, we did not include this date in Figure 3b.

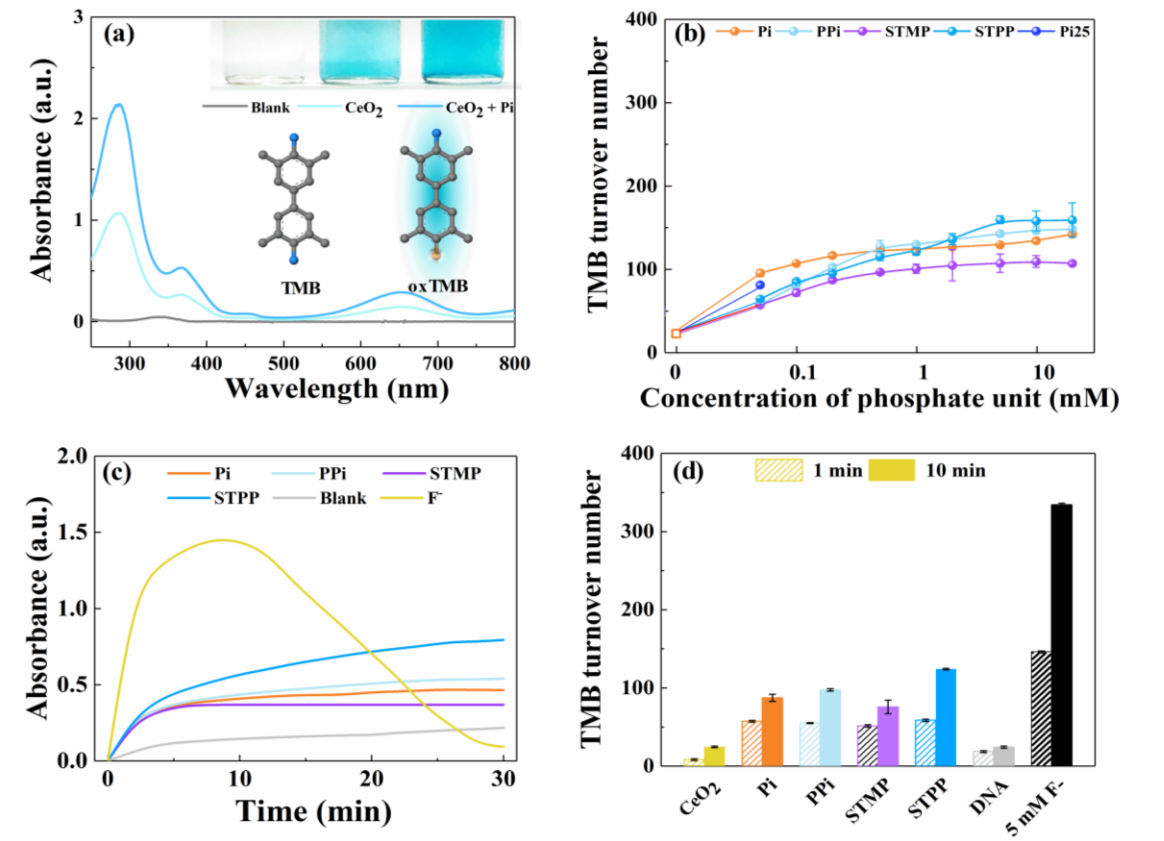

Figure 3. (a) UV-vis spectra of TMB oxidation by the CeO_2 nanoparticles without or with Pi (10 mM) after 30 min reaction. Inset: the structures and photographs of TMB before and after oxidation. (b) Turnover number of TMB oxidation by CeO_2 in the presence of various concentrations of the phosphates (total phosphate unit concentration plotted) after 60 min reaction. (c) Kinetics of TMB oxidation in the presence of CeO_2 by 10 mM total phosphate unit of different species monitored at 652 nm. Fluoride (5 mM) was included as a control group. (d) Turnover number of each species based on the data in (c) for reacting for 1 and 10 min. TMB (0.5 mM), CeO_2 nanoparticles (100 μg/mL), and acetate buffer (10 mM, pH 4) were used in all reactions.

From the kinetic data (Figure 3c), the highest reaction rate was still observed with F^-, which even showed the two-electron product as indicated by the drop of the 652 nm peak.[13] STPP was the next highest, followed by PPi, Pi and STMP. Oxidation of TMB by the bare CeO_2 was fast only in the first 2 min, and then the reaction became much slower. In the following 10 min, <20 oxTMB were produced by each bare CeO_2. In the presence of 10 mM Pi, ~80 oxTMB were converted by each CeO_2 nanoparticle after 10 min, which was 4-fold of that of the bare CeO_2 (Figure 3d). Since TMB is positively charged, the effect can be easily explained by an electrostatic attraction of the substrate to the phosphate-capped nanozyme surface.

DNA can both enhance and inhibit CeO_2 activity depending on buffer and DNA concentration. After studying the phosphates, we then turned our attention to DNA oligonucleotides. Since different buffers were used in the previous literature (Table S1), we also compared acetate and phosphate buffers. We first studied the effect of DNA concentration (Figure 4a). In pH 4 phosphate buffer, with 100 μg/mL (430 nM) CeO_2, the color change of TMB without DNA was small. In contrast, the A_{15} DNA functionalized CeO_2 showed stronger activity for TMB oxidation reflected from a more intense blue color. By adding 50 nM of A_{15} DNA, the reaction rate was the highest, while further increase of the DNA led to slower reaction. The turnover numbers by each CeO_2 nanoparticle after reaction 60 min are shown in Figure 4b. Our observation was consistent with Andreescu's report when the concentration of DNA was below 50 nM DNA, after which our system showed inhibition while continued increase was observed by Andreescu et al. The concentration of the CeO_2 used was similar (100 or 120 μg/mL).[34] However, in Andreescu's report, the buffer and pH were not specified. In addition, we used different DNA sequences and CeO_2 nanoparticles, and it is hard to make further comparison.

We noticed that our samples precipitated during the reaction and this was attributed to the phosphate buffer. Precipitation can also bring in fluctuations in the measurement and affect the catalytic activity. The effect of CeO_2 aggregation by duplex DNA was attributed to the decreased activity in a few reports.[31-32] Note that at the optimal DNA concentration of 50 nM, less than the concentration of the CeO_2 (430 nM). The overall effect of DNA was quite moderate. Thus, it is unlikely that the effect of DNA was acting on individual CeO_2 nanoparticles, but to affect other aspects such as the aggregation of CeO_2 (*vide infra*). We observed the promotion effect with the DNA, but not with polyphosphate (Figure S5). Therefore, DNA bases should have played some role in this process such as the promoted adsorption of the TMB substrate.

We then repeated the test in acetate buffer (Figure 4c). In this case, the effect of DNA was insignificant, until 10 μM DNA was added, when the reaction was slightly inhibited. The turnover numbers by each CeO_2 nanoparticle after reaction 60 min is shown in Figure 4d. We further studied the effect of DNA sequence and length, where 50 nM of 5, 15 and 30-mer of various DNA all showed a similar level of enhancement for activity in phosphate buffer (Figure 4e), while the

activity remained largely constant with 5 μM DNA in the acetate buffer (Figure 4f). Since the effect of DNA length was quite small, most likely no all phosphates in the backbone were adsorbed.

Therefore, the type of buffer also affected the effect of DNA, with a moderate promotion effect in phosphate buffer at low DNA concentrations. In acetate buffer, the effect was from none to moderate inhibition at high DNA concentrations. Normally, we avoid using phosphate buffer for CeO_2 (or other metal oxides) since phosphate can strongly adsorb on its surface and compete with DNA adsorption. For example, Pi, PPi, STPP, STMP and Pi_{25} could displace the adsorbed DNA at neutral pH.[36]

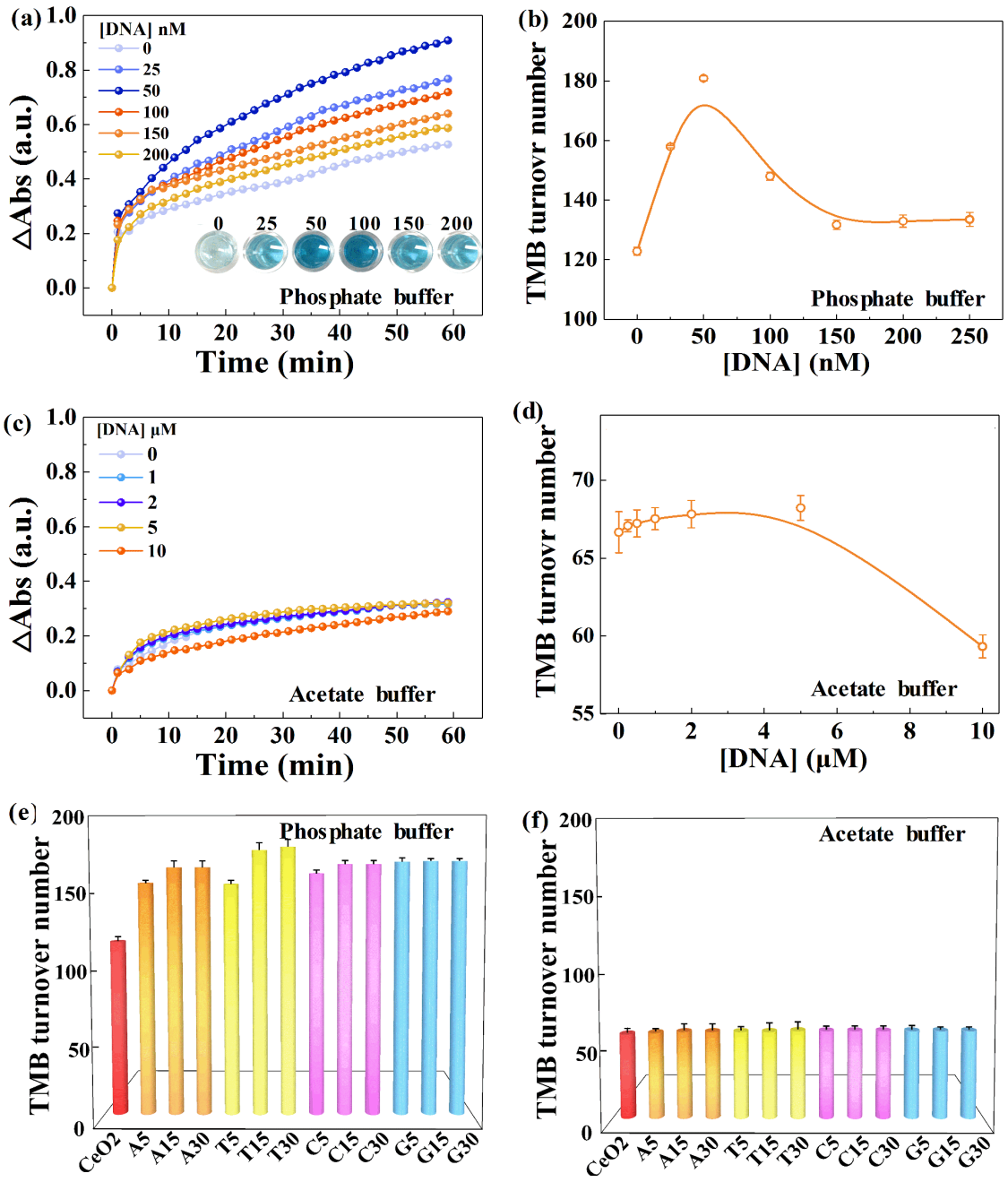

Figure 4. Oxidation kinetics of TMB (1 mM, 652 nm) by 100 μg/mL CeO_2 nanoparticles in 10 mM pH 4 (a) phosphate and (c) acetate buffer. The photograph in (a) shown the color changed of TMB oxidation on a screening plate containing 0, 25, 50, 100, 150 and 200 nM of A_{15} DNA after 60 min reaction. (b, d) Turnover number of TMB by each CeO_2 nanoparticles after 60 min reaction. Oxidation of TMB as a function of DNA sequence and length in (e) phosphate and (f) acetate buffer. The concentration of DNA was 50 nM in phosphate buffer and 5 μM in acetate buffer.

DNA adsorption by CeO_2 nanoparticles in different buffers. To further study the mechanism, we followed the adsorption of DNA on CeO_2 nanoparticles in different conditions. For DNA to affect the catalytic activity, it is likely that DNA needs to adsorb on the CeO_2 surface. CeO_2 nanoparticles adsorb DNA via the negatively charged phosphate backbone.[29, 34] The zeta-potential of DNA-Functionalized CeO_2 nanoparticles in different buffers was measured. In phosphate buffer, the CeO_2 nanoparticles were always negatively charged from pH 3 to pH 8 due to adsorption of phosphate (Figure 5a). Although phosphate-capped CeO_2 was expected to repel DNA, we still measured DNA adsorption. We mixed a fixed concentration of a Cy3-labeled DNA (Cy3-C_{15}) with various concentrations of CeO_2 nanoparticles in phosphate buffer (pH 4, 10 mM), where fully quenched fluorescence was observed at high CeO_2 concentrations suggesting DNA adsorption (Figure 5b). After centrifugation and dispersing the pellets in pH 7 phosphate buffer, the DNA desorbed with fluorescence recovery (Figure 5c). Although adsorption of phosphate gave negatively charged surface, the CeO_2 nanoparticles were still able to adsorb negatively charged DNA in pH 4 phosphate buffer.

For comparison, in acetate buffer, the CeO_2 nanoparticles were positively charged at low pH (Figure 5a). After adsorption of 50 nM DNA, the zeta-potential remained positive until the pH was greater than 5. As shown in Figure 1d (blue trace), 50 nM DNA cannot fully neutralize the surface charge on the CeO_2, which can explain the positive charge observed here.

We then quantitatively measured DNA adsorption in different buffers (Figure 5d). In the acetate buffer, the fluorescence of Cy3-labeled DNA was quenched immediately, confirming that almost all DNA strands were adsorbed. Although carboxylate was shown to adsorb on CeO_2, the affinity was quite weak and cannot inhibit the adsorption of DNA.[38-40] Acetate was not able to displace adsorbed DNA.[29] In the phosphate buffer, DNA adsorption was slower although adsorption was still achieved. We also measured DNA adsorption as a function of pH in phosphate

buffer (Figure 5e). Interestingly, about 50% fluorescence from the DNA was quenched, which means about 50% DNA adsorbed in the pH 4 phosphate buffer. DNA adsorption was gradually inhibited when pH increased from 4 to 7. Thus, pH had a great effect on DNA adsorption on the CeO_2 nanoparticles in phosphate buffer. To further confirm this, we compared phosphate-induced DNA desorption at pH 4 and pH 7.6 (Figure S6). With 1 mM phosphate, no DNA desorbed at pH 4, while 40% DNA desorbed at pH 7.6. With 10 mM phosphate, more than 20% of pre-adsorbed DNA still remained on the surface of CeO_2, also indicating that DNA can better compete with phosphate at low pH.

We also noticed aggregation of the CeO_2 nanoparticles in phosphate buffer in the presence of DNA. We quantitatively studied it using DLS (Figure 5f). With 50 nM DNA, the CeO_2 nanoparticles had the smallest average size and best dispersion. Adding more than 50 nM DNA started to cause more aggregation of the CeO_2 nanoparticles, and the catalytic activity also decreased. Such aggregation might also contribute to the decreased activity. In contrast, in acetate buffer, the particle size was always smaller than 15 nm (Figure 5g).

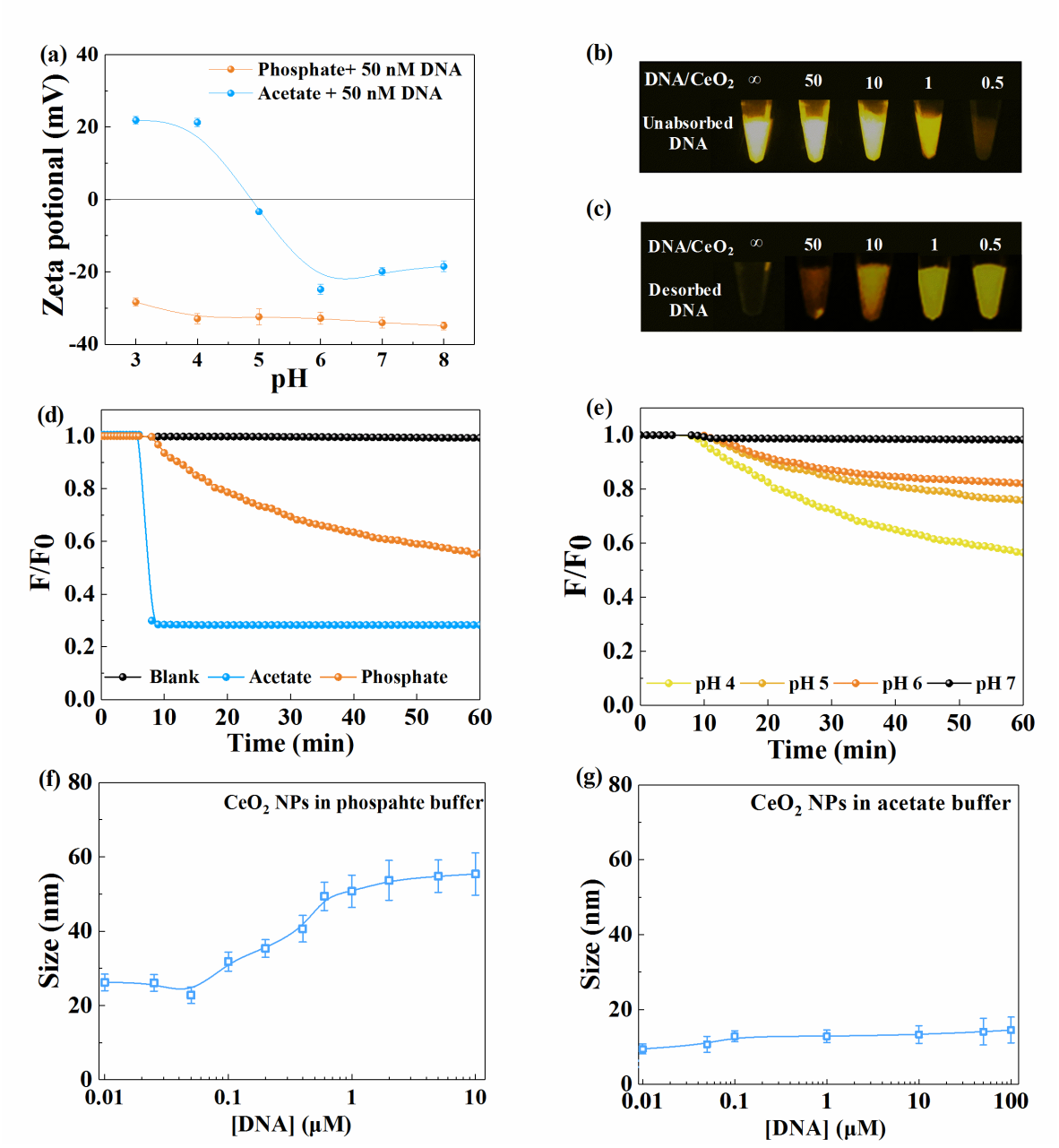

Figure. 5 (a) Zeta-potential of the CeO_2 nanoparticles before and after adding DNA (50 nM) in different buffers at different pH. (b) Photograph of Cy3-C_{15} and CeO_2 mixed at various ratios in pH 4 phosphate buffer, and (c) released Cy3-C_{15} from the CeO_2 nanoparticles after centrifugation and then dispersed in pH 7 phosphate buffer. The numbers on each tube are the molar ratio between the DNA and CeO_2 nanoparticles, where the first tube on the left did not contain any CeO_2. Quenching of Cy3-C_{15} by the CeO_2 nanoparticles (d) in different buffers, and (e) in phosphate buffer (10 mM) of different pH. CeO_2 nanoparticles size change after adding various DNA in (f) phosphate, and (g) acetate buffer.

Figure 6 shows the TEM micrographs of DNA-modified CeO_2 nanoparticles in different conditions, and the results were consistent with the DLS data. With 50 nM DNA in phosphate

buffer, the average size was ~20 nm in Figure 6a. Under this condition, the oxidase-like activity of the CeO_2 enhanced slightly compared to the bare CeO_2 (an average particle size of ~5 nm). However, the size increased to about 50 nm in the presence of 200 nM DNA (Figure 6b), and the activity decreased. In acetate buffer, the particle size of the CeO_2 was less than 20 nm in both DNA concentrations (Figure 6 c, d).

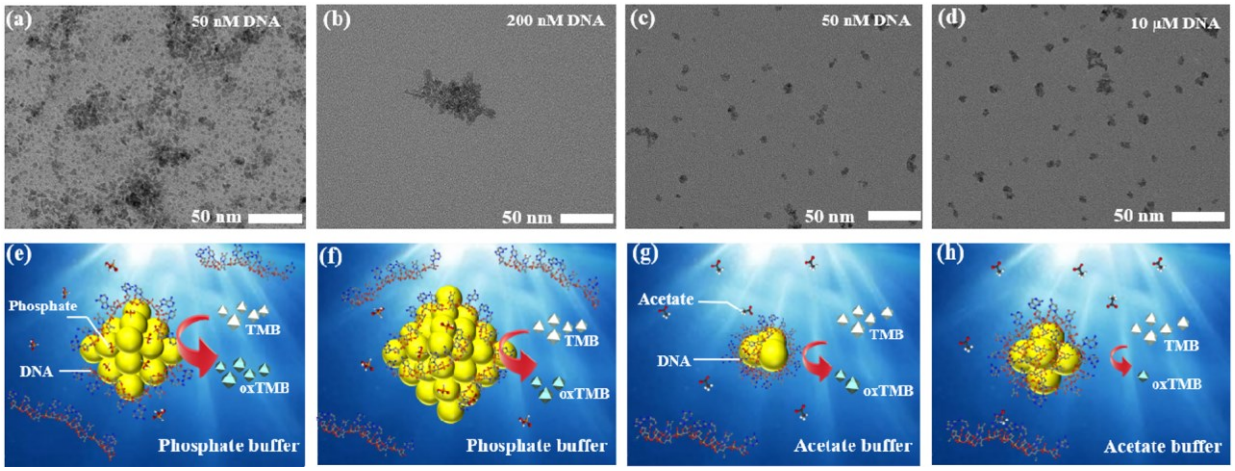

Figure 6. TEM micrographs of the CeO_2 nanoparticles in phosphate buffer upon adding (a) 50 nM of DNA and (b) 200 nM of DNA; and in acetate buffer upon adding (c) 50 nM of DNA and (d) 10 μM of DNA. Cartoons showing that the CeO_2 nanoparticles can tightly adsorb phosphate, resulting in negatively charged surface, but they have a low affinity with acetate. In phosphate buffer, the oxidase-like activity was (e) slightly improved by adding 50 nM DNA, while (f) less improved with 200 nM DNA. (g) In acetate buffer, the oxidase activity was not much affected by 50 nM of DNA, (h) but the activity was slightly inhibited upon adding 10 μM of DNA.

Based on this work, we rationalized the effect of DNA adsorption on the catalytic activity of the CeO_2 nanoparticles in different buffers. Since Pi and polyphosphate can all enhance the activity of CeO_2 (100 μg/mL, 430 nM) for the oxidation of TMB, at a low DNA concentration of 50 nM, DNA may act as a polyphosphate to enhance the activity in phosphate buffer (Figure 6e). Since DNA can still be adsorbed in pH 4 phosphate buffer, it indicates a strong DNA/CeO_2 interaction, and thus DNA may compete with phosphate to exert its enhancement function as a polyphosphate at pH 4. With further increased DNA concentration (200 nM), the CeO_2 nanoparticles aggregated more, likely due to crosslinking of multiple CeO_2 nanoparticles by DNA. The aggregation and the

steric effect of the adsorbed DNA may balance the promotion effect of DNA as a polyphosphate; thus, no more enhancement was observed (Figure 6f).

In the acetate buffer, the CeO_2 nanoparticles were better dispersed with a smaller average particle size. A low concentration DNA of 200 nM was efficiently adsorbed, balancing the activation role as a polyphosphate (e.g. attracting TMB substrate) and the inhibition role as a surface blocker (Figure 6g). When the DNA concentration was too high (10 μM), the adsorbed DNA was over saturated (Figure 6h), and the blocking effect dominated yielding a moderate inhibition occurred. Overall, DNA did not have much effect on catalysis in the acetate buffer.

Implications of this work.

From this study, we can see that the activity of the CeO_2 nanozyme can be affected by many factors. If we only discuss the phosphate species, the activity is also highly related to pH, charge of the substrate and length of the polyphosphate. Many different observations have been made in the literature for the effect of DNA on CeO_2. It is highly important that research groups publishing work after carefully searching the literature and quantitatively discuss the difference in experimental conditions, so that to avoid contradiction in results and confusing readers. It is also very important to report detailed experimental conditions such as the type of buffer, salt concentration and pH.

CeO_2 nanoparticles are not the only example. Many other nanozymes have been reported to be accelerated or inhibited by DNA. In our previous work, DNA-capped iron oxide nanoparticles were nearly 10-fold more active as a peroxidase mimic for TMB oxidation than the naked nanoparticles.[41] The activity was also affected by DNA length, sequence, concentration and pH. Yigit *et.al* investigated the peroxidase-like activity of citrate-capped gold nanoparticles for TMB oxidation.[42] This effect can be fine-tuned by altering the nucleotide components of the DNA sequence and length, and by changing the reaction parameters (H_2O_2 concentration, pH and buffer).[43-44] These examples also indicate the importance of specifying the detailed experimental conditions.

Finally, to test these systems for analytical applications, one would have to be careful when calling them sensors. At least for the current system, the activity was affected by many factors and the amount of signal change was in general small in the presence of DNA.

Conclusions

In this work, we systematically studied five types of phosphates including Pi, PPi, STTP, STMP, Pi_{25}, and also DNA oligonucleotides of various lengths and sequences. On one hand, phosphates can only moderately enhance ABTS oxidation, and this effect was especially small for Pi. On the other hand, phosphates accelerate oxidation of TMB more. We only observed a moderately increased activity by a low concentration of DNA in phosphate buffer. The activity was not affected much by DNA in the acetate buffer, except when the DNA concentration was very high. Therefore, the promotion and inhibition of the oxidase-mimicking activity of nanoceria in different condition can be affected by many factors, and the conditions need to be carefully specified and researched to obtain consistent results.

Acknowledgement

Funding for this work was from the Natural Sciences and Engineering Research Council of Canada (NSERC), and the National Natural Science Foundation of China (21838001, 21525625 and 31961133018), and the National Key Research and Development Program of China (2018YFA0902200). Y. Zhao was supported by a China Scholarship Council (CSC) scholarship to visit the University of Waterloo.

References

[1] H. Wei, E. Wang, *Chem. Soc. Rev.* **2013**, *42*, 6060-6093.

[2] Y. Huang, J. Ren, X. Qu, *Chem. Rev.* **2019**, *119*, 4357–4412.

[3] Y. Zhou, B. Liu, R. Yang, J. Liu, *Bioconjugate Chem.* **2017**, *28*, 2903-2909.

[4] R. Zhang, K. Fan, X. Yan, *Sci. China Life Sci.* **2020**, DOI: https://doi.org/10.1007/s11427-019-1570-7.

[5] L. Gao, J. Zhuang, L. Nie, J. Zhang, Y. Zhang, N. Gu, T. Wang, J. Feng, D. Yang, S. Perrett, X. Yan, *Nat. Nanotechnol.* **2007**, *2*, 577-583.

[6] A. Asati, S. Santra, C. Kaittanis, S. Nath, J. M. Perez, *Angew. Chem. Int. Ed.* **2009**, *48*, 2308-2312.

[7] C. Xu, X. Qu, *NPG Asia Mater.* **2014**, *6*, e90.

[8] I. Celardo, J. Z. Pedersen, E. Traversa, L. Ghibelli, *Nanoscale* **2011**, *3*, 1411-1420.

[9] A. Kumar, S. Das, P. Munusamy, W. Self, D. R. Baer, D. C. Sayle, S. Seal, *Environ. Sci. Nano* **2014**, *1*, 516-532.

[10] F. Chen, M. Bai, K. Cao, Y. Zhao, J. Wei, Y. X. Zhao, *Adv. Funct. Mater.* **2017**, *27*.

[11] D. Li, B. Liu, P.-J. J. Huang, Z. Zhang, J. Liu, *Chem. Commun.* **2018**, *54*, 12519-12522.

[12] Y. Chang, M. Liu, J. Liu, *Anal. Chem.* **2020**, *92*, 3118-3124.

[13] B. Liu, Z. Huang, J. Liu, *Nanoscale* **2016**, *8*, 13562-13567.

[14] T. Pirmohamed, J. M. Dowding, S. Singh, B. Wasserman, E. Heckert, A. S. Karakoti, J. E. S. King, S. Seal, W. T. Self, *Chem. Commun.* **2010**, *46*, 2736-2738.

[15] E. G. Heckert, A. S. Karakoti, S. Seal, W. T. Self, *Biomaterials* **2008**, *29*, 2705-2709.

[16] Z. Tian, T. Yao, C. Qu, S. Zhang, X. Li, Y. Qu, *Nano Lett.* **2019**, *19*, 8270-8277.

[17] T. Yao, Z. Tian, Y. Zhang, Y. Qu, *ACS Appl. Mater. Interfaces* **2019**, *11*, 195-201.

[18] F. Xu, Q. Lu, P.-J. J. Huang, J. Liu, *Chem. Commun.* **2019**.

[19] H. Cheng, S. Lin, F. Muhammad, Y.-W. Lin, H. Wei, *ACS Sensors* **2016**, *1*, 1336-1343.

[20] Y. Wang, T. Liu, J. Liu, *ACS Appl. Nano Mater.* **2020**, *3*, 842-849.

[21] S. Singh, T. Dosani, A. S. Karakoti, A. Kumar, S. Seal, W. T. Self, *Biomaterials* **2011**, *32*, 6745-6753.

[22] B. Liu, J. Liu, *Nano Res.* **2017**, *10*, 1125–1148.

[23] H. Cheng, Y. Liu, Y. Hu, Y. Ding, S. Lin, W. Cao, Q. Wang, J. Wu, F. Muhammad, X. Zhao, D. Zhao, Z. Li, H. Xing, H. Wei, *Anal. Chem.* **2017**, *89*, 11552-11559.

[24] X. Wang, Y. Hu, H. Wei, *Inorg. Chem. Front.* **2016**, *3*, 41-60.

[25] D. Li, S. L. Garisto, P.-J. J. Huang, J. Yang, B. Liu, J. Liu, *Inorg. Chem. Commun.* **2019**.

[26] Y. Zhao, Y. Wang, A. Mathur, Y. Wang, V. Maheshwari, H. Su, J. Liu, *Nanoscale* **2019**.

[27] B. Liu, J. Liu, *Chem. Commun.* **2014**, *50*, 8568-8570.

[28] F. Wang, J. Liu, *Small* **2014**, *10*, 3927-3931.

[29] R. Pautler, E. Y. Kelly, P.-J. J. Huang, J. Cao, B. Liu, J. Liu, *ACS Appl. Mater. Interfaces* **2013**, *5*, 6820–6825.

[30] D. Yang, M. Fa, L. Gao, R. Zhao, Y. Luo, X. Yao, *Nanotechnology* **2018**, *29*, 385101.

[31] M. I. Kim, K. S. Park, H. G. Park, *Chem. Commun.* **2014**, *50*, 9577-9580.

[32] H. Y. Kim, J. K. Ahn, M. I. Kim, K. S. Park, H. G. Park, *Electrochem. Commun.* **2019**, *99*, 5-10.

[33] C. Xu, Z. Liu, L. Wu, J. Ren, X. Qu, *Adv. Funct. Mater.* **2014**, *24*, 1624-1630.

[34] G. Bülbül, A. Hayat, S. Andreescu, *Adv. Healthcare Mater.* **2016**, *5*, 822-828.

[35] X. Wang, B. Liu, J. Liu, *Langmuir* **2018**, *34*, 15871-15877.

[36] X. Wang, A. Lopez, J. Liu, *Langmuir* **2018**, *34*, 7899-7905.

[37] B. Liu, Z. Sun, P.-J. J. Huang, J. Liu, *J. Am. Chem. Soc.* **2015**, *137*, 1290-1295.

[38] A. S. Karakoti, P. Yang, W. Wang, V. Patel, A. Martinez, V. Shutthanandan, S. Seal, S. Thevuthasan, *J. Phys. Chem. C* **2018**, *122*, 3582-3590.

[39] S. Sanghavi, W. Wang, M. I. Nandasiri, A. S. Karakoti, W. Wang, P. Yang, S. Thevuthasan, *Phys. Chem. Chem. Phys.* **2016**, *18*, 15625-15631.

[40] Z. Lu, A. Karakoti, L. Velarde, W. Wang, P. Yang, S. Thevuthasan, H.-f. Wang, *J. Phys. Chem. C* **2013**, *117*, 24329-24338.

[41] B. Liu, J. Liu, *Nanoscale* **2015**, *7*, 13831-13835.

[42] M. S. Hizir, M. Top, M. Balcioglu, M. Rana, N. M. Robertson, F. S. Shen, J. Sheng, M. V. Yigit, *Anal. Chem.* **2016**, *88*, 600-605.

[43] S. Wang, W. Chen, A.-L. Liu, L. Hong, H.-H. Deng, X.-H. Lin, *ChemPhysChem* **2012**, *13*, 1199-1204.

[44] J. Yang, Y. Lu, L. Ao, F. Wang, W. Jing, S. Zhang, Y. Liu, *Sensor. Actuat. B: Chem.* **2017**, *245*, 66-73.

10.1002/cbic.202000049

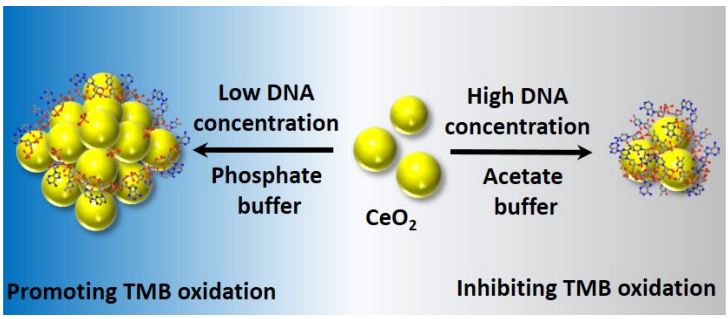

The oxidase-like activity of nanoceria can be promoted by phosphate and polyphosphate, while the effect of DNA depends on its concentration, the type of buffer and substrate, while the sequence of DNA is less important.